Available online at www.sciencedirect.com
ScienceDirect
International Journal of Fatigue 30 (2008) 528–537
International Journal of Fatigue
www.elsevier.com/locate/ijfatigue

Fatigue design of cast steel nodes in tubular bridge structures

S.C. Haldimann-Sturm [a,*], A. Nussbaumer [b]

[a] Swiss Federal Railways SBB, Infrastructure – Civil Engineering, Schanzenstr. 5, CH-3000 Bern 65, Switzerland
[b] Ecole Polytechnique Fédérale de Lausanne EPFL, Steel Structures Laboratory ICOM, GC B3 505, Station 18, CH-1015 Lausanne, Switzerland

Received 7 August 2006; received in revised form 11 February 2007; accepted 19 March 2007
Available online 27 March 2007

Abstract

Due to their aesthetic and structural advantages, tubular space truss structures are enjoying increasing popularity in modern bridge construction. The use of cast steel nodes for the joints between the circular hollow section members is also becoming increasingly popular. The fatigue design of such joints, however, requires additional knowledge with respect to their fatigue resistance. Previous experimental investigations showed very clearly that the fatigue behaviour is governed by the welds between the casting stubs and the hollow section members. This paper presents a methodology for the determination of allowable initial sizes of casting defects as a function of the required fatigue resistance of the welds. The relative influence of the main parameters is quantitatively discussed and recommendations for design are given.

Keywords: Cast steel; Connection; Casting defect; Fatigue design; Bridge; Tube

1. Introduction

Due to their aesthetic and structural advantages, tubular space truss structures are enjoying increasing popularity in modern bridge construction. In a rising number of theses bridges, cast steel nodes for the joints between the circular hollow section members are used. The fatigue design of such joints, however, requires additional knowledge with respect to their fatigue resistance. The present paper deals with the global fatigue behaviour of cast steel nodes used in longitudinal truss girders of steel–concrete composite bridges.

The global fatigue behaviour of cast steel nodes in a truss girder was quantified by Haldimann–Sturm [1,2] on the basis of experimental investigations. The relative influence of the resistance of the cast steel node and the resistance of the girth butt welds was analysed as a function of various parameters. The experimental results showed very clearly that the fatigue behaviour was governed by the welds in all tested configurations. The fatigue resistance of the cast nodes could never be mobilized. It was concluded that a lower casting quality level than what is usually specified today would be sufficient to meet the fatigue requirements of cast steel nodes in modern bridge construction. The casting quality level is defined by the smallest casting defect size which is to be detected by non-destructive testing. Lowering the required casting quality level would reduce the fabrication cost of cast steel nodes. An economically optimal fatigue design consists, therefore, of adapting the fatigue resistance of the cast node to that of the welds. The present paper concentrates on the adaptation of the resistance of the cast steel nodes to the resistance of the welds. This can be done by defining allowable initial casting defect sizes as a function of the required fatigue resistance of the welds.

It is clear that the overall fatigue resistance would benefit most from an improvement in the fatigue resistance of the girth butt welds. Their fatigue behaviour was investigated in a research program conducted simultaneously to ours by Veselcic et al. [3]. For the same design life, an

* Corresponding author. Tel.: +41 51 220 67 01; fax: +41 51 220 50 14.
E-mail address: senta.haldimann@sbb.ch (S.C. Haldimann-Sturm).

0142-1123/$ - see front matter © 2007 Elsevier Ltd. All rights reserved.
doi:10.1016/j.ijfatigue.2007.03.007

improved fatigue resistance of girth butt welds would allow the wall thicknesses of the tubular members to be reduced. The wall thicknesses of the cast steel nodes could thus be reduced as well, which means smaller allowable initial defect sizes.

Using a numerical boundary element model, the allowable initial casting defect sizes were calculated for cast steel nodes in a typical steel–concrete composite bridge. Since the stress intensity geometric correction factor is known as a constant for a crack embedded in an infinite solid ($2/\pi$ in the case of a circular crack), it was studied if the results of the numerical investigations could be approximated by a constant as well. This was indeed the case, allowing the procedure for the fatigue design of cast steel nodes to be simplified considerably. It gives the procedure a general applicability for this type of bridges.

A parametric study was performed. The influence of the traffic and fatigue loads, of the cast steel fracture toughness, of the yield strength and of the node dimensions on the allowable initial defect size was investigated. For a range of node dimensions, assuming a fracture toughness likely to be encountered in practice, mean traffic and fatigue loads, the allowable initial casting defect sizes were quantified.

2. Numerical study

2.1. Numerical investigation on cast steel nodes of a typical tubular bridge

A numerical study was made to quantify allowable initial sizes of defects in cast nodes that provide a balanced design between the various potential crack initiation sites, especially between the girth butt welds and the cast steel node. As a basis for the numerical study, a typical steel–concrete road bridge was defined taking into account the properties of existing tubular bridge structures described by Schlaich et al. [4] and Veselcic et al. [5].

When designing the shape of a node, attention must be paid to the volume shrinkage caused by the cooling of the molten steel. The volume shrinkage must be compensated by a suitably designed feeder. In order to avoid solidification cracks, wall thicknesses should increase continuously towards the feeder with a minimum angle of 4°. The length of a region with constant wall thickness should not exceed three times the wall thickness. The node shape should always be defined in collaboration with the foundry, which is as well responsible for the design of the feeder by means of solidification simulations.

Fig. 1 shows the geometry and the structural model of the typical bridge. The shape of the cast steel nodes, used for the typical bridge, was chosen such that the outer diameter of the stubs corresponds to the outer diameter of the truss members. The wall thickness at the stub ends is governed by the fatigue strength of the girth butt welds. For this typical bridge, the girth butt welds were assumed to have backing bars. Such a weld has a fatigue strength of

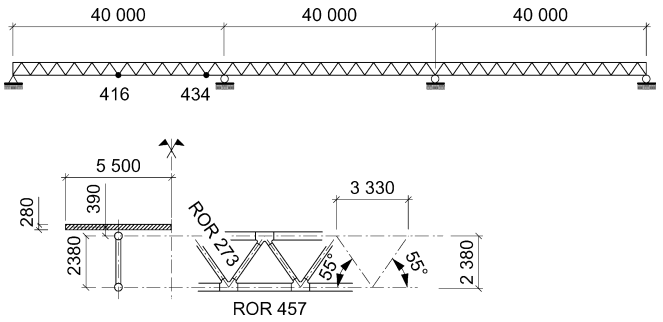

Fig. 1. Geometry and structural model of the typical tubular truss bridge (dimensions in mm).

87 MPa at 2×10^6 cycles according to fatigue tests by Haldimann-Sturm [1]. The wall thickness of the node stubs was increased with an angle of 4° towards the node centre. As in existing node shapes, round corners are put between the casting stubs.

A numerical boundary element (BE) model of the cast steel node was made using the commercial software BEASY®. It was used to simulate the propagation of a crack initiating from a casting defect. Due to the longitudinal symmetry, only one half of the cast steel node had to be modelled. In the symmetry plane, the out-of-plane displacement u was constrained. In the chord stub where $z > 0$, all displacements were constrained (Fig. 2). The internal forces acting on the casting stubs were applied as stresses. The plausibility of these boundary conditions was verified by Haldimann-Sturm [1] by comparing the principal strains obtained from the BE model with the measured strains found in experiments.

The forces acting on the cast steel node were calculated for the fatigue limit state (FLS) and the ultimate limit state

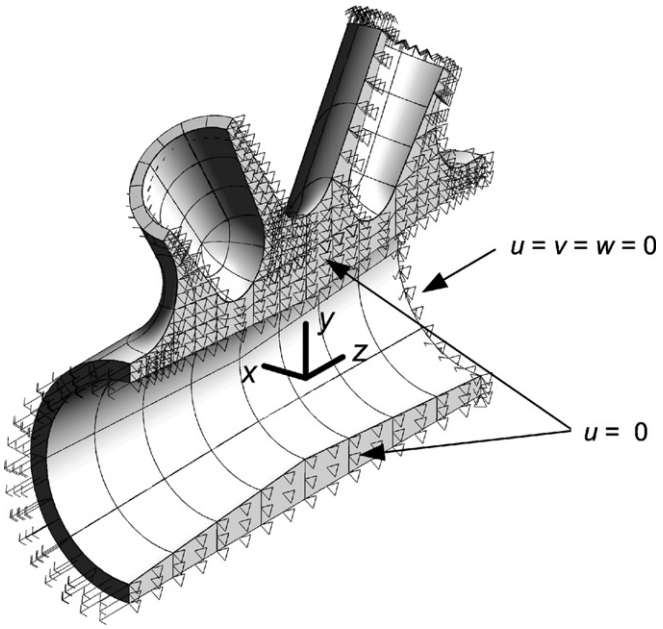

Fig. 2. Boundary conditions of the BE cast node model.

(ULS), using the Swiss design code SIA 261 [6] and a simple bar model of the typical steel–concrete road bridge. The Swiss design code is close to the Eurocodes, the design made is thus similar to one made using the Eurocodes. For example, it uses the same load model as the fatigue load model 1 in EN1991-2 [7], but with a slightly different intensity. The bridge is assumed to be located on a main road (0.5×10^6 trucks/direction/year). The study was limited to the two most critical nodes in the bridge: one at midspan and one near an intermediate support, where the axial brace forces are much higher (nodes 416 and 434 in Fig. 1). The configuration of the forces acting on the casting stubs is very different between these two nodes.

The casting defects were modelled as two-dimensional circular cracks of radius a_0, which are assumed to represent all types of casting defects. This is a very conservative assumption, as the fatigue behaviour of a two-dimensional crack is much more critical than that of casting defects like gas holes, slag inclusions or shrink holes. Fig. 3 shows nine different locations i in the node where the allowable initial sizes of casting defects should be quantified. At location 7, an internal crack was assumed. At all other locations, the more critical surface cracks were introduced in the cast node model. The internal crack dimensions correspond to half of the axes of an ellipse, a and c. In the case of a surface crack, a is the crack depth and c is one half of its length on the surface.

The position of the fatigue load model on the bridge, where the stress intensity factor (SIF) at the different defect locations reaches its maximum and minimum, is a priori unknown, but required in order to quantify allowable initial defect sizes. Therefore, SIF influence lines have to be calculated. This was done for an identical crack at all locations in the node by transferring the internal forces history that result from the moving fatigue load on the structural bridge model into the BE node model. From the influence line of the SIF and the crack propagation plane, the two load positions defining the range of the stress intensity factor $\Delta K_I(a)$ for modus I could be determined. For these two load positions, the internal forces acting on the casting stubs were extracted from the bridge model and introduced into the BE node model. The use of only two loading sets without any phase effects simplifies the crack propagation simulations.

Crack propagation in the node was simulated using the boundary element software package BEASY®. The results are given at intermediate steps in terms of crack configuration, crack depth a and the corresponding maximum and minimum stress intensity factors $K_{I,max}$ and $K_{I,min}$ (Fig. 4 shows $K_{I,max}$). The crack propagation simulation was stopped shortly before the crack depth reached the wall thickness at the defect location.

The three steps of the procedure for the numerical investigation on the allowable initial crack size a_0 are summarized in Fig. 5.

In the first step, the critical crack size a_{crit}, for which fracture (either brittle, with tearing or by plastic collapse) can be excluded, has to be found. This is possible by using the failure assessment diagram (FAD) from Milne et al. [8], see also [9]. To be able to use this diagram, the stress intensity factor in the ultimate limit state $K_{I,ULS}$ and a reference stress $\sigma_{ref}(a)$ are needed. $K_{I,ULS}$ was calculated with the aid of the BE models containing the crack configuration of each intermediate crack propagation step and by applying the forces calculated with the structural bridge model and the ultimate static load. The FAD has to be used with the maximum of the stress intensity factor $K_{I,ULS}$ at the crack edge c and at the crack depth a. The numerical results showed that the maximum stress intensity factor occurred at the crack edge (Fig. 6 shows $K_{I,ULS}$ maxima).

The reference stress $\sigma_{ref}(a)$ was calculated in the cross-section reduced by the present crack. Finally, the stress intensity factor $K_r(a)$ is normalised by the toughness K_{Ic} and the stress $L_r(a)$ is normalised by the average stress $\sigma_f(a)$ of the yield strength f_y and the tensile strength f_u.

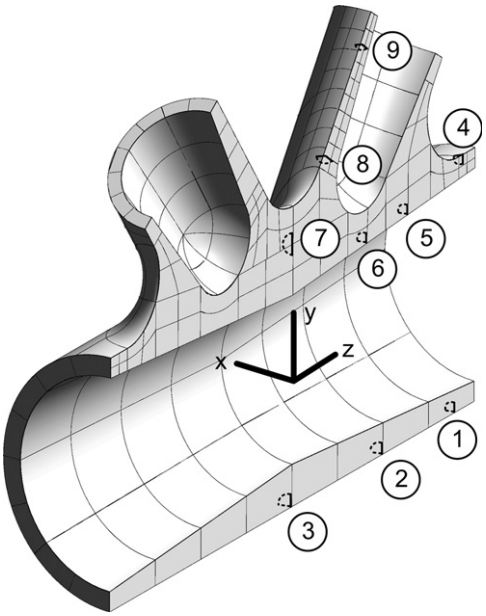

Fig. 3. Casting defect locations.

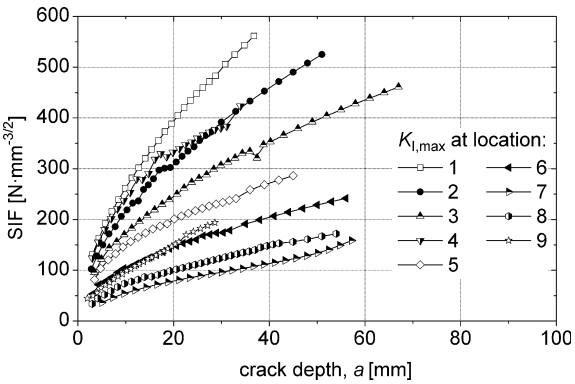

Fig. 4. SIF $K_{I,max}$ results for the node at midspan (node 416).

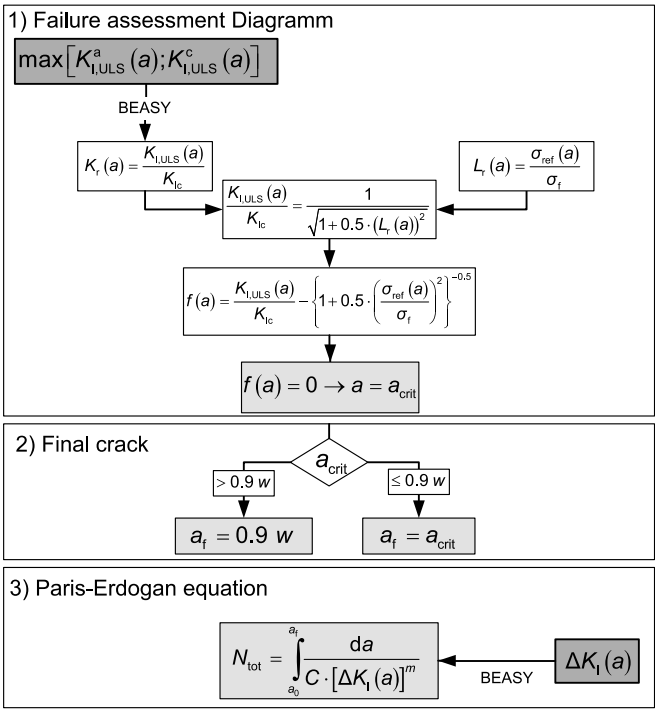

Fig. 5. Steps of the procedure for the numerical investigation on casting defects in cast steel nodes of a typical tubular bridge.

From these quantities, the critical crack size a_{crit} can be determined.

Although it does not mean failure, a through-thickness crack is deemed unacceptable for a cast steel node in bridge structures. For this reason, an additional failure criterion, $a_f < 0.9w$ (w is the wall thickness at the crack location), is introduced in a second step. Accordingly, the final crack depth a_f corresponds to the minimum of the critical crack size a_{crit} and $0.9w$.

In a third step, once a_f is known, the allowable initial crack size a_0 can be calculated using the Paris–Erdogan equation backwards. As the BEASY® output for crack propagation simulations consists of discrete stress intensity factor values (Fig. 4), the Paris–Erdogan equation can only be solved discretely:

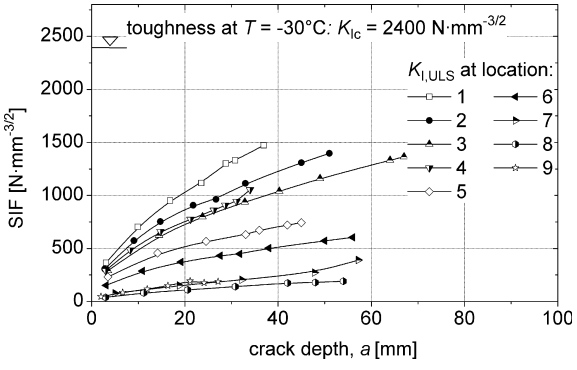

Fig. 6. SIF $K_{I,ULS}$ maxima (at the crack edge c) for the node at midspan (node 416).

$$N_{tot} = \sum_{k=0}^{n-1} \Delta N_k = \frac{1}{C} \cdot \left[\frac{a_1 - a_0}{\Delta K_{I,0}^m} + \frac{a_2 - a_1}{\Delta K_{I,1}^m} + \cdots + \frac{a_n - a_{n-1}}{\Delta K_{I,n}^m} \right] \quad (1)$$

Using Eq. (1), the allowable initial crack size a_0 can be found:

$$a_0 = a_1 - \Delta K_{I,0}^m \cdot \left[N_{tot} \cdot C - \left(\frac{a_2 - a_1}{\Delta K_{I,1}^m} + \cdots + \frac{a_n - a_{n-1}}{\Delta K_{I,n}^m} \right) \right] \quad (2)$$

N_{tot} service life in terms of the number of loading cycles (determined by the welds)

$\Delta K_{I,k}$ difference in stress intensity factor for the propagation step k

C Paris law constant, $C = 2 \times 10^{-13}$ (mm/cycle) (N mm$^{-3/2}$)$^{-m}$

m crack propagation parameter, $m = 3$

a_n final crack depth a_f

k number of available data points from the propagation simulation

The determination of the allowable initial defect size is based on the following assumptions:

- According to Blair and Stevens [10], the crack propagation parameters for cast steel are equal to those of ferritic–perlitic steel.
- A service life of 70 years has been assumed according to the Swiss design code SIA 261 [6]. (*Note*: Eurocode EN1993-2 recommends a service life of 100 years.) The fatigue loads are adapted to correspond to a service life of 2×10^6 cycles.
- The initial defects are assumed to behave as long cracks. For that reason, the crack initiation period is not taken into account for the service life.
- Deterministic calculations are done.
- For the fracture verification, the fracture toughness under quasi-static loading is used, as well as the nominal yield and ultimate stress values.

The relevant failure criterion of the second step in the procedure was always the prevention of a through-thickness crack. The results showed that with this condition, a node containing cracks does never fracture nor attain plastic collapse. Fig. 6 shows that the stress intensity factor in the ultimate limit state $K_{I,ULS}$ never reaches its critical value, i.e. the minimum material toughness of 2400 N mm$^{-3/2}$.

With the SIF results presented in Figs. 4 and 6 and by applying the above-mentioned procedure, the allowable initial defect sizes were calculated using a spreadsheet program. A summary of the results is given in Table 1. The allowable initial defect sizes were found to be very large for the typical steel–concrete composite bridge. They range

Table 1
Allowable initial defect sizes at the different locations of the cast node 416

Location i	Wall thickness w_i (mm)	$a_{0,i}$ (mm)	$a_{0,i}/w_i$ (%)
1	41.0	11.5	28
2	55.9	22.2	40
3	75.0	41.7	56
4	38.7	14.1	36
5	49.0	34.9	71
6	61.9	49.8	81
7	63.5	55.9	88
8	59.1	41.1	70
9	31.6	16.1	51

from approximately 28% to 88% of the wall thickness at the defect location. The smallest allowable defect size was found in the casting stub at location 1, the biggest at location 7 between the two braces of the node at midspan (node 416).

2.2. Generalisation of numerical results

A further step of the numerical investigation consists in the analysis of the SIF values, aiming at a generalization and simplification of the procedure to determine the allowable initial crack sizes in cast steel nodes that was employed for the typical tubular truss bridge. This simplified procedure should enable an engineer to estimate the allowable initial crack size (and therewith the defect size) without carrying out numerical crack propagation simulations, but only stress analysis.

In general, the correction factor Y depends, among others, on the position of the crack in the node and on the crack shape. But in certain cases, like an internal crack in an infinite solid, it is a constant. In our case, it was found that simplification can also be achieved by expressing the stress intensity factor $K_I(a)$ with a constant correction factor Y:

$$K_I(a) = Y \cdot \sigma_1 \sqrt{\pi \cdot a} \quad (3)$$

σ_1 major principal stress at defect location
a depth of the surface crack

The constant correction factor Y was obtained by normalising the SIF with the principal stress at the location i. Fig. 7 shows the normalised SIF in function of the square root of the depth $\sqrt{a}$, together with the regression curve that was used to determine the constant correction factor.

Table 2 summarises the values of the constant correction factor in the crack depth Y_a and in the crack length Y_c. The factors Y_a for a two-dimensional internal crack and for a surface crack are close to the theoretical values. As Y_c is higher than Y_a, the surface crack's length increases faster than its depth.

An error on the correction factor has a considerable influence on the allowable initial defect size as the correction factor in Eq. (3) is raised to the power of $m = 3$ in the Paris–Erdogan equation (step 3 in Fig. 5). Comparison of the allowable initial defect sizes obtained from the numerical SIF and from the constant correction factors shows a deviation of less than ±20% (Fig. 8). The constant correction factor being a mean value of the numerical results, the deviation can be positive or negative.

In view of the other uncertainties, e.g. on the loading side, and of the significant simplification that is introduced by using the same constant correction factor for all defect locations, this deviation is considered to be acceptable. The determination of the allowable initial defect sizes is now straightforward thanks to the simplified procedure.

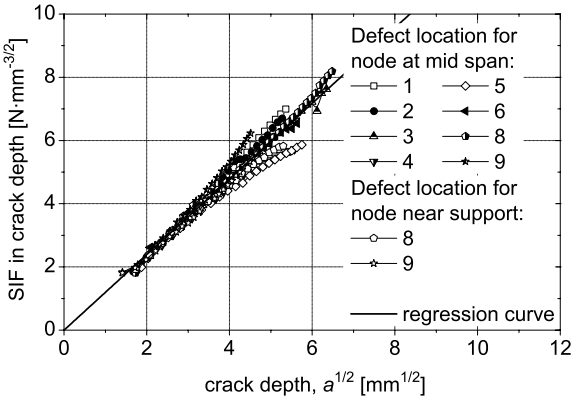

Fig. 7. Normalised SIF at different surface crack locations in the node at midspan and near the support.

Table 2
Constant correction factor at crack depth and length

Type of crack	Mean value		Theoretical value
	Y_a	Y_c	Y_a
Internal crack	0.62	0.64	$2/\pi$
Surface crack	0.67	0.77	$1.1 \cdot 2/\pi$

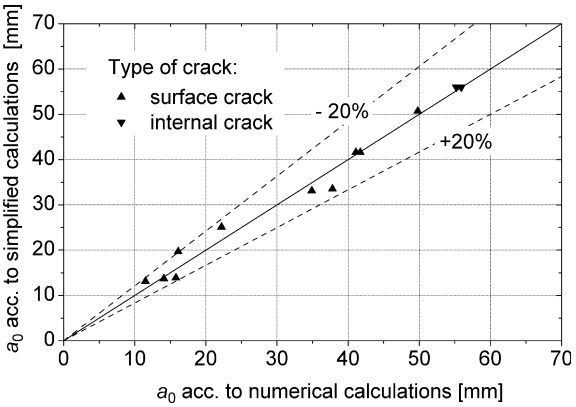

Fig. 8. Comparison of the allowable initial defect sizes obtained by numerical calculations and by using the simplified procedure.

3. General procedure for the fatigue design

Due to the introduction of the constant correction factor Y, the engineer is now able to estimate the allowable

initial defect sizes for the critical cast steel nodes of the bridge without running time-consuming numerical crack propagation simulations.

First of all, one must decide how many different quality levels (and therewith different allowable initial defect sizes) are admitted per cast steel node. Non-destructive testing (NDT) is required to assure a certain quality level. The better the quality level is, the higher are the NDT costs. A gradation in quality levels is therefore advisable if costs should be reduced.

For each node region with a different quality level, the maximum and minimum major principal stresses under fatigue load (for $\Delta\sigma_{1,E2}$) and the major principal stress under ultimate static load ($\sigma_{1,Ed}$, necessary for the fracture design with the minimum service temperature of the structural member to be taken into account as leading action and the traffic model as accompanying action) must be calculated by using a 3D finite or boundary element model of an uncracked node. The design casting defect's location corresponds to the location of the maximum major principal stress. The forces acting on the cast steel node can be calculated using a bar model of the bridge.

The calculation steps required to find the allowable initial defect size have already been explained for the typical tubular truss bridge. The introduction of the constant correction factor affects steps 1 and 3 in Fig. 9 (rectangles with dark grey background).

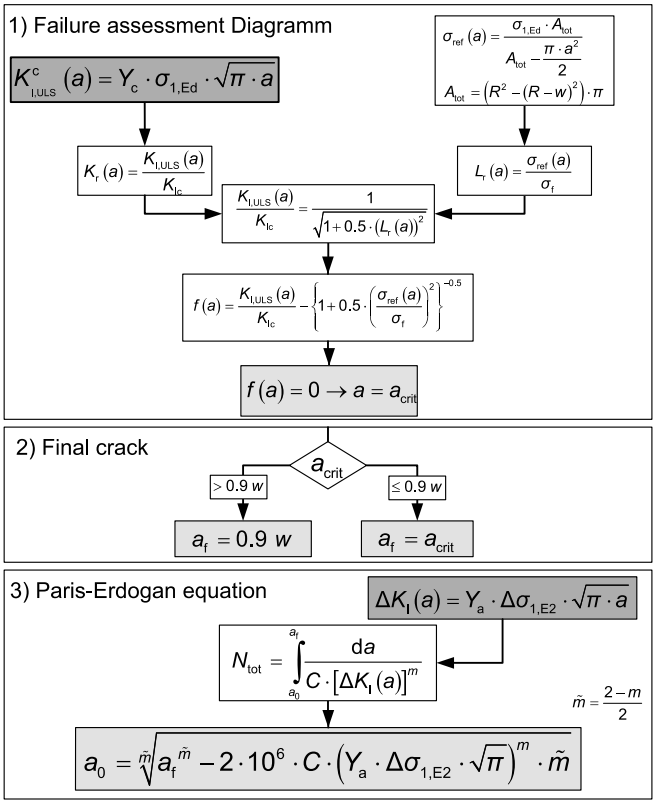

Fig. 9. Calculation steps of the simplified procedure.

In order to determine the critical crack size for the brittle fracture criterion, the reference stress $\sigma_{ref}(a)$ in the cross-section weakened by the crack has to be calculated. For this purpose, two main assumptions are made. The cross-section A_{tot} containing the casting defect is considered to be a circular cross-section (radius R) with the wall thickness w equal to the thickness at the position of the defect in the node. The stress in the cross-section is assumed to be uniform and to correspond to the maximum major principal stress $\sigma_{1,Ed}$ in the 3D model of the uncracked node. As the maximum stress intensity factor $K_{I,ULS}(a)$ is required in order to use the FAD, the stress intensity factor for the ultimate limit state $K_{I,ULS}$ is calculated by using the constant correction factor Y_c.

Once the final crack size a_f is known, the allowable initial crack size a_0 can be calculated using the Paris–Erdogan equation. In contrast to the preceding case, this equation can now be solved for a_0 without iteration. As crack propagation is considered in the direction of the wall thickness, the difference of the stress intensity factor used in the Paris–Erdogan equation is calculated using Y_a.

The simplified procedure can be implemented as an algorithm. This has been done as a user-friendly function for Microsoft Excel®, written in Visual Basic for Applications (VBA). With the aid of this algorithm, the allowable initial defect sizes can be calculated for any cast steel node without running crack propagation simulations. For the complete algorithm, see Haldimann–Sturm [1].

4. Parametric study

The algorithm described above is suitable to perform a parametric study in order to determine the influence of the following parameters on the allowable initial defect size of cast steel defects:

- utilisation ratio under ultimate static load (ULS) and under fatigue load (FLS), defined as the ratios between the applied stresses and the yield strength of the cast steel:

$$\chi_{ULS} = \sigma_{1,Ed}/f_y \quad (4)$$

$$\chi_{FLS} = \Delta\sigma_{1,E2}/f_y \quad (5)$$

- fracture toughness, K_{Ic}, and yield strength, f_y, of the cast steel.

The results of the parametric study are not tabulated, as the values can be calculated for each specific case with the help of the algorithm. It is, however, interesting to get a qualitative overview.

4.1. Influence of the main parameters on the allowable initial defect size

The loading state of the cast steel node is defined by the utilisation ratio χ_{ULS} in the ultimate limit state and the util-

isation ratio χ_{FLS} in the fatigue limit state. The first-mentioned is required for the fracture design with the minimum service temperature of the structural member to be taken into account as leading action and the traffic model as accompanying action. Fig. 10 shows the influence of the two utilisation ratios for one specific case on the final crack size a_f and on the allowable initial defect size a_0 ($\gamma = D/2w = 2$, wall thickness $w = 100$ mm, diameter $D = 400$ mm, yield strength $f_y = 355$ MPa, fracture toughness of the cast steel $K_{Ic} = 2000$ N mm$^{-3/2}$). In this case, the final crack size results from the brittle fracture criterion within the entire (χ_{FLS}, χ_{ULS})-range, such that $a_f = a_{crit}$. It can be seen from the figure that the final crack size depends on the utilisation ratio χ_{ULS} mainly. For a constant ratio χ_{ULS}, the allowable initial defect size decreases with increasing utilisation ratio χ_{FLS}. When determining a_0, the stress range $\Delta\sigma_{1,E2} = \chi_{FLS} \cdot f_y$ is raised to the power of $m = 3$ in the Paris–Erdogan equation. That is why the influence of the stress range is exponential when determining a_0 from a_f. It can be concluded that, at high utilisation ratios χ_{FLS}, ultimate limit state stresses do not influence the allowable initial defect size a_0. At low χ_{FLS} values, however, these stresses have a strong influence on a_0.

If the fracture toughness is increased to, let us say, $K_{Ic} = 3000$ N mm$^{-3/2}$ (Fig. 11), the final crack size a_f, and therefore also a_0, reaches its maximum within the range of $0.45 \leqslant \chi_{ULS} \leqslant 0.6$ and is now limited by the criterion of 90% of the wall thickness at the defect location. When comparing Figs. 10 and 11, an increasing influence of the fracture toughness at very low χ_{FLS} values is observed. The minimum K_{Ic} value for which the utilisation ratio χ_{ULS} has no more influence can also be found. For a toughness $K_{Ic} = 3900$ N mm$^{-3/2}$ or above, the final crack size, and consequently the allowable initial defect size, is at its maximum value over the entire χ_{ULS} range. In conclusion, it is generally not possible to benefit from good (high) fracture toughness in terms of large allowable initial defects sizes. The only exceptions are cases where the utilisation ratio in the fatigue limit state χ_{FLS} is very low.

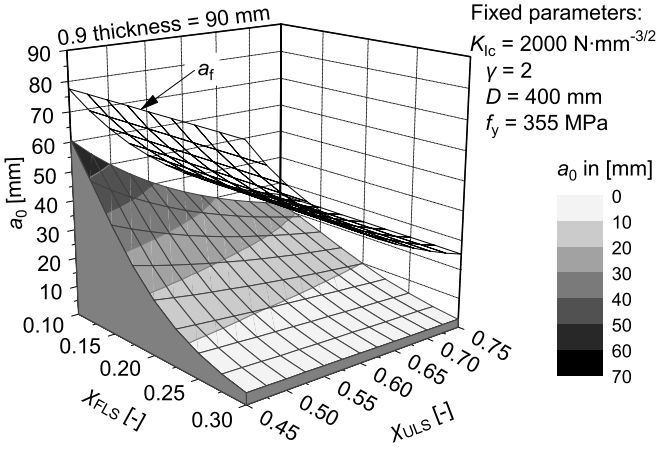

Fig. 10. Influence of the ULS and FLS utilisation ratios ($K_{Ic} = 2000$ N mm$^{-3/2}$) on a_0.

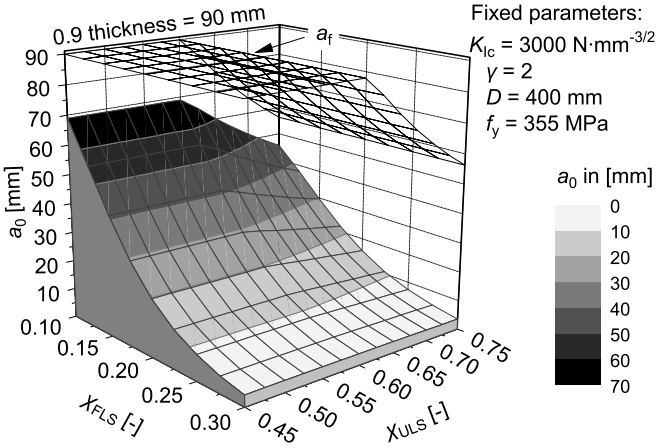

Fig. 11. Influence of the ULS and FLS utilisation ratios ($K_{Ic} = 3000$ N mm$^{-3/2}$) on a_0.

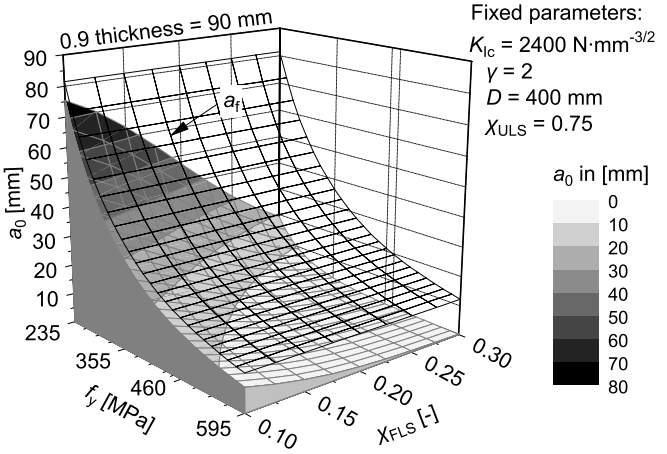

Fig. 12. Influence of the yield strength on a_0.

Fig. 12 illustrates the influence of the yield strength f_y on the allowable initial defect size a_0. Since the choice of using a material of higher strength is dictated by the wish to carry higher loads and/or have more slender elements, it was assumed that an increase of the yield strength causes an increase of the stress for the fracture criterion $\sigma_{1,Ed} = \chi_{ULS} \cdot f_y$ and the fatigue stress range $\Delta\sigma_{1,E2} = \chi_{FLS} \cdot f_y$. For this reason, a_0 and a_f decrease with increasing yield strength when χ_{FLS} is held constant. A structural member is assumed to be dimensioned for an optimum ultimate limit state utilisation ratio of $\chi_{ULS} = 0.75$, which corresponds to the case where the traffic model is taken as accompanying action at the minimum service temperature (leading action). If higher yield strength steel is chosen for the structural member, the fatigue stress range increases as a result of the reduced wall thickness. The utilisation ratio χ_{FLS}, however, remains constant. The smaller wall thickness leads to a smaller final crack size. That is why the allowable initial crack size decreases with increasing yield strength as a result of the increase of $\Delta\sigma_{1,E2}$ and the decrease of a_f. Consequently, higher yield strength does

not necessarily increase a structure's lifetime in the case of large fatigue stress ranges.

4.2. Allowable initial defect size for mean utilisation ratios of the node

To provide the interested reader with general idea, the possible range of a_0 is in the following estimated based on a set of plausibly chosen fracture toughness values, typical ULS (χ_{ULS}) and FLS (χ_{FLS}) utilisation ratios as well as cross-sections (γ, D). A probable fracture toughness values (and not the required characteristic value) is used. The evaluation of (unpublished) Charpy test results from tests carried out at −30 °C by the German foundry Friedrich Wilhelms–Hütte GmbH gives a mean value of 103 J with a standard deviation of 17 J. The test results fit well to a normal distribution. The correlation between the Charpy impact resistance and the fracture toughness is described by different empirical equations. The most conservative equation is given by Sailors and Corten [11]:

$$K_{Ic,Test} = 466 \cdot \sqrt{A_v} \quad (6)$$

A_v Charpy impact resistance (J)
$K_{Ic,Test}$ fracture toughness (N mm$^{-3/2}$) at test temperature −30 °C

With the data at hand, this yields $K_{Ic,Test} = 4700$ N mm$^{-3/2}$.

To keep the figures simple, single mean values of the ULS and of the FLS utilisation ratios are chosen: $\chi_{ULS} = 0.2$, $\chi_{FLS} = 0.6$.

Figs. 13 and 14 illustrate the allowable initial defect size as a function of the dimensions γ and D for two typical yield strength values f_y. It can be seen that for $f_y = 355$ MPa and over the entire range of γ and D, the initial defect size a_0 ranges from 6.3 mm to 23.6 mm. In the case of $f_y = 460$ MPa, it is $3.4\text{ mm} \leqslant a_0 \leqslant 8.3$ mm. When using these values for a specific application, it is important to bear in mind that constant utilisation ratios have been assumed for the entire node. In reality, the utilisation ratio can vary from stub to stub in a node and different quality levels are often specified for different zones in a node.

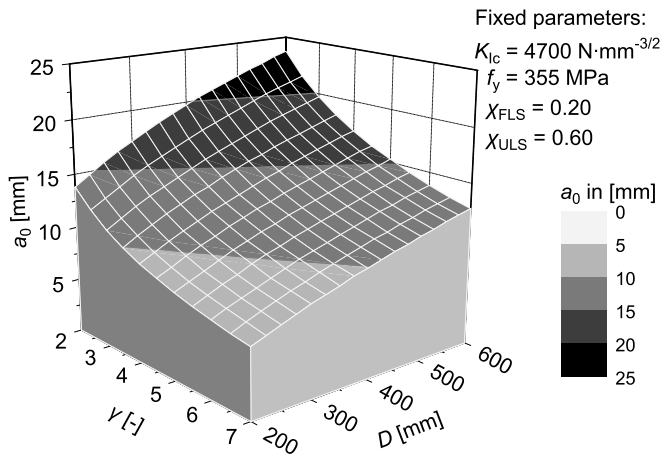

Fig. 13. Allowable initial defect size as a function of the cross-section dimensions for $f_y = 355$ MPa.

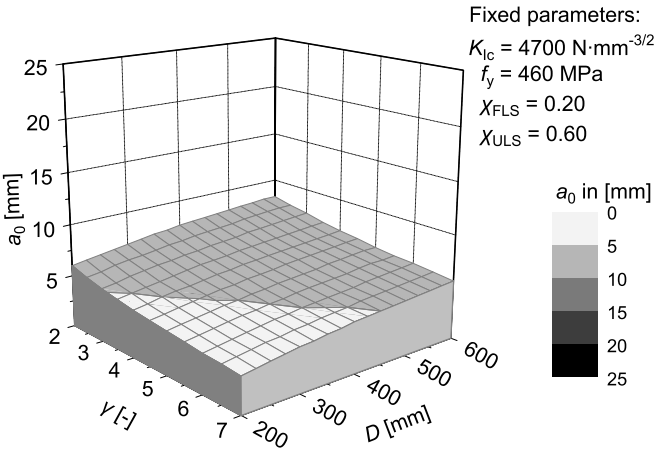

Fig. 14. Allowable initial defect size as a function of the cross-section dimensions for $f_y = 460$ MPa.

Due to technical casting requirements, the wall thickness of the central part of the cast steel node must be much higher than the thickness of the casting stub ends. The utilisation ratio decreases towards the node's centre due to the increasing wall thickness. In common K and KK nodes (nodes with two and four diagonals), the cross-section with the maximal wall thickness of 150 mm (corresponds to the lower limit $\gamma = 2$ and the upper limit $D = 600$ mm) is located in the central part of the node. In this cross-section, utilisation ratios are generally far below the assumed values of $\chi_{ULS} = 0.2$ and $\chi_{FLS} = 0.6$. Consequently, the allowable initial defect sizes are significantly higher than the upper limits given above (23.6 mm for $f_y = 355$ MPa and 8.3 mm for $f_y = 460$ MPa).

A cross-section with $\gamma = 7$ and $D = 200$ mm, which corresponds to a wall thickness of $w = 14$ mm, is likely to be located close to the casting stub ends. Compared with this wall thickness, the lower limits of the allowable initial defect sizes (6.3 mm for $f_y = 355$ MPa and 3.4 mm for $f_y = 460$ MPa) are very large.

For application in practice, it is recommended to calculate for each different cast node the allowable initial defect sizes by means of the algorithm given by Haldimann-Sturm [1].

4.3. Detectability of the allowable initial defect sizes

Once the allowable initial defect sizes have been determined by computation, it is very important that they can be detected by non-destructive testing. It would not make sense to specify defect sizes which cannot be detected. In the fatigue verification, no defect sizes below the detection limit should be considered. In Table 3, the detection limits of defects for different testing methods are summarized.

Table 3
Overview of defect detection limits of non-destructive testing methods according to Blumenauer [12]

Testing method	Detection limit[b]	
	Defect depth	Defect length
Radiographic	>0.4–2% of wall thickness	
Ultrasonic	Defect echo > 2 × microstructure signal Defect depth > 3 × surface roughness	
Magnetic particle[a]	>10 μm	>100 μm
Liquid penetrant[a]	>20 μm	>1 mm

[a] Only surface defects.
[b] Standard values for actual testing methods.

For radiographic testing, magnetic particle testing and liquid penetrant testing, quantitative absolute or relative detection limits are given. For ultrasonic testing, it is more complicated since the detection limit increases with increasing surface roughness. The detection limit is at least threetimes the casting surface roughness, provided that the defect echo is not less than twice the microstructure echo (interference level). According to standards like DIN 1690-2:1985 [13], EN 12680-1:2003 [14] or EN 12680-2:2003 [15], the casting surfaces should enable a perfect interface to the transceiver. This is guaranteed as long as the casting surfaces correspond to the visual tactile comparators according to the standard EN 1370:1996 [16]. The surface parameters that are required to determine the surface roughness, such as the roughness height, the mean roughness or the profile depth cannot be determined by means of the visual tactile comparators. The roughness height of these visual tactile comparators is in the range of micrometers, but precise values are not available. Christianus et al. [17] explain that the original idea of specifying numerical surface roughness values e.g. for different cast methods or cast materials was dropped during the development of the European standard EN 1370:1996 [16]. To be able to give precise values, more investigations would be required.

In addition to the surface roughness, the testability of castings by ultrasonic means depends on the material microstructure and the wall thickness. For this reason, the standards DIN 1690-2:1985 [13], EN 12680-1:2003 [14] and EN 12680-2:2003 [15] require the testability of castings by ultrasonic to be judged by comparing the echo height of a reference reflector (an idealized defect, a perfect hole with a defined diameter) to the interference level due to the material's microstructure. To ensure good testability, the echo height of the reference reflector must exceed the interference level by 6 dB. When testing a casting, the echo of a reflecting location is compared to the echo of the reference reflector. If the latter is higher, the location is declared as a defect. The echo height does, however, not provide information on the defect type nor its size in the wall thickness direction. Size and shape of the defect will rarely correspond to the reference reflector. Further investigations are required in order to assess to what extent defects that are smaller than the reference reflector can be detected in practice.

The smallest detectable reference reflector is specified as a function of the wall thickness of the casting. The reference reflector with a diameter of 2 mm should, for example, be detectable for a highly stressed casting with a wall thickness $\leqslant$100 mm according to the standard EN 12680-2:2003 [15]. The standard does, however, not specify what highly stressed means in terms of the utilisation ratio. For the casting stub ends, a reference reflector with a diameter of 1.5 mm should be detectable. In an additional inspection instruction, the foundry and the customer can specify even smaller reference reflectors. The allowable initial defect sizes given for medium utilisation ratios (Figs. 13 and 14) are larger than the diameter of these reference reflectors. Allowable initial defects should, therefore, be detectable. In view of the uncertainties discussed above, it should nevertheless be verified carefully whether this is truly the case.

5. Summary and conclusions

Based on the numerical study on cast steel nodes of a typical tubular bridge and on the parametric study, the following conclusions can be drawn:

- A procedure to quantify the allowable initial casting defect sizes that ensure a balanced design between the various potential crack initiation sites in a cast steel node was developed for a typical steel–concrete composite bridge. The defect sizes range from approximately 28% to 88% of the wall thickness at the defect's location.
- The procedure was simplified by the use of an approximate formulation of the stress intensity factor that is based on a constant correction factor. By virtue of this simplification, the procedure could be implemented as an algorithm available to everyone.
- In the case of high stress amplitudes in the fatigue limit state, the allowable initial defect size is independent of the stresses in the ultimate limit state (traffic load model).
- It is generally not possible to benefit from good (high) fracture toughness in terms of large allowable initial defects sizes. The only exceptions are cases where the stress amplitudes in the fatigue limit state are very low.
- The use of steel with higher yield strength does not necessarily increase a structure's lifetime in the case of large fatigue stress ranges.
- The algorithm yields the allowable initial defect sizes between 6.3 mm and 23.6 mm for the yield strength $f_y = 355$ MPa and between 3.4 mm and 8.3 mm for $f_y = 460$ MPa over a wide range of cross-section dimensions and for mean stress amplitudes of $0.2f_y$ at fatigue limit state and for mean stresses of $0.6f_y$ at ultimate limit state.
- For the implementation of the proposed procedure in practice, the relationship between the reference reflector size and the computed initial defect size should be spec-

ified. Allowable defect sizes that are lower than the detection limit of the non-destructive testing method shall not be specified.

List of symbols

a	one-half the dimension of the first axis of an internal elliptical crack or depth of a surface crack
c	one half the dimension of the second axis of an internal elliptical crack or one half of the crack's length on the surface
χ_{FLS}	utilisation ratio under fatigue load, $\chi_{FLS} = \Delta\sigma_{1,E2}/f_y$
χ_{ULS}	utilisation ratio under ultimate load, $\chi_{ULS} = \sigma_{1,Ed}/f_y$
f_y	yield strength
$\sigma_{1,Ed}$	major principal stress at the defect location under ultimate load (traffic load model)
$\Delta\sigma_{1,E2}$	amplitude of the major principal stress at the defect location under fatigue load
γ	geometric parameter, $\gamma = D/2w$
D	outer diameter of the casting stub
w	wall thickness at the defect location

Acknowledgements

The research results presented in this paper are the outcome of a doctoral thesis [1] that was done at the Steel Structures Laboratory ICOM at Ecole Polytechnique Fédérale de Lausanne EPFL. The authors thank Prof. Dr. Manfred A. Hirt, director of ICOM and supervisor of the thesis, for his support. The research is part of the project P591 "Wirtschaftliches Bauen von Strassen- und Eisenbahnbrücken mit Stahlhohlprofilen" which is directed by the Versuchsanstalt für Stahl, Holz und Steine at the Technische Universität Karlsruhe (Germany). The research was supported both financially and with academic advice by the Forschungsvereinigung Stahlanwendung e.V. (FOSTA), Düsseldorf (Germany) and the Stiftung Stahlanwendungsforschung, Essen (Germany). Parts of the study were furthermore financially supported by the Swiss National Science Foundation (SNF). All financial and scientific contributions are highly appreciated.

References

[1] Haldimann-Sturm SC. Ermüdungsverhalten von Stahlgussknoten in Brücken aus Stahlhohlprofilen. PhD thesis, EPFL no. 3274, Ecole polytechnique fédérale de Lausanne (EPFL), December 2005. Algorithm as a user-friendly function for Microsoft Excel® can also be downloaded.

[2] Sturm S, Nussbaumer A, Hirt MA. Fatigue behaviour of cast steel nodes in bridge structures. In: Proceedings of the 10th international symposium on tubular structures. Tubular structures X. Madrid: A.A. Balkema Publishers; 2003. p. 357–64.

[3] Veselcic M, Herion S, Puthli R. Selection of butt-welded connections for joints between tubulars and cast steel nodes under fatigue loading. In: Packer JA, Willibald S, editors. Proceedings of 11th International Symposium and IIW International Conference on Tubular Structures. Tubular Structures XI. Québec City, Canada: Taylor & Francis Group; 2006. p. 585–92.

[4] Schlaich J, Schober H. Rohrknoten aus Stahlguss. Stahlbau, vol. 68(8). Berlin: Ernst & Sohn; 1999. p. 652–65.

[5] Veselcic M, Herion S, Puthli R. Cast steel in tubular bridges – new applications and technologies. In: Proceedings of the 10th international symposium on tubular structures. Tubular structures X. Madrid: A.A. Balkema Publishers; 2003. p. 135–42.

[6] SIA 261. Einwirkungen auf Tragwerke. Schweizerischer Ingenieur- und Architektenverein, 2003.

[7] prEN 1991-2:2002. Actions on structures. Part 2: Traffic loads on bridges. CEN, January 2002.

[8] Milne I, Ainsworth RA, Dowling AR, Stewart AT. Assessment of the integrity of structures containing defects. R/H/R6 – Revision 3, Central Electricity Generating Board, May 1986.

[9] BRITISH STANDARD INSTITUTE BSI. Guide on methods for assessing the acceptability of flaws in metallic structures, 2000.

[10] Blair M, Stevens TL. Steel castings handbook. Steel Founders' Society of America and ASM International; 1995.

[11] Sailors RH, Corten HT. Relationship between material fracture toughness using fracture mechanics and transition temperature tests. In: Proceedings of the 1971 fifth national symposium on fracture mechanics, Urbana-Champaign, IL, ASTM STP 514, No. Part II, 31 August–2 September 1971. p. 164–91.

[12] Blumenauer H. Technische Bruchmechanik. Deutscher Verlag für Grundstoffindustrie, Leipzig, Germany, 1993. ISBN 3-342-00659-5.

[13] DIN 1690-2:1985. Technische Lieferbedingungen für Gusstücke aus metallischen Werkstoffen. DIN, June 1985.

[14] EN 12680-1:2003. Founding. Ultrasonic examination. Steel castings for general purposes. CEN, March 2003.

[15] EN 12680-2:2003. Founding. Ultrasonic examination. Steel castings for highly stressed components. CEN, March 2003.

[16] EN 1370:1996. Founding – Surface roughness inspection by visual tactile comparators. CEN, January 2003.

[17] Christianus D, Herfurth K. Europäische Normung: Prüfung der Oberflächenrauheit mit Hilfe von Vergleichsmustern – DIN EN 1370. konstruieren + giessen, vol. 23(4), 1998. p. 26–30.